State-of-the-art of crack propagation modelling in tubular joints

IOP Conf. Series: Materials Science and Engineering **700** (2019) 012035 doi:10.1088/1757-899X/700/1/012035

State-of-the-art of crack propagation modelling in tubular joints

M Atteya*, O Mikkelsen and H G Lemu

Dept. of Mechanical and Structural Engineering and Materials Science, University of Stavanger, Norway

* Corresponding author: mostafa.a.atteya@uis.no

Abstract. Offshore structures are conventionally designed for a service life between 20-30 years and mostly used beyond their service life. They are operated up to the point where costs of operations, maintenance and repair exceed the revenue generated by the offshore structure. The cyclic nature of environmental loading induces multi-axial stresses with high gradients in welded tubular joints that lead to fatigue cracks emanating from imperfections in the welded materials. Tubular joints may exhibit significant residual life after fatigue cracks formation due to crack propagating around the weld circumference. It is important to understand tubular joints behaviour and estimate the residual life beyond crack initiation as it promotes the safe operation of the offshore installation, inspection planning and life extension of the asset. This paper presents an overview of the residual life estimation of cracked tubular joints using numerical methods. The recent developments and possible enhancements to the modelling methods of cracked tubular joints are presented.

1. Introduction

In fracture mechanics theory, fatigue life is generally divided into three stages, namely, crack initiation, crack propagation and final failure, though the traditional S-N curves based fatigue design methods make no clear distinction between crack initiation and crack propagation. For tubular joints, fatigue life may be divided broadly into four stages from N_1 to N_4: N_1 is the point at which the crack is first noted by any inspection method, N_2 denotes the first visual crack, N_3 denotes through-thickness crack, and N_4 represents the actual failure of the joint. Failure may be defined as the appearance of through-thickness crack (N_3) as the available experimental data showed that it is difficult to conclude N_4 from S-N curves [1-4]. Tubular joints may exhibit significant residual life after through-thickness crack formation due to crack propagating around the weld circumference. Zhang and Stacey [2] reported that for a total of 281 test results the mean ratio between N_4/N_3 is 1.38. Residual life of damaged joints depends on joint type, chord thickness, loading mode, as well as environmental exposures. It is important to understand tubular joints behavior and estimate the residual life beyond crack initiation as it promotes the safe operation of the offshore installation, inspection planning and life extension of the asset [2].

The behavior of cracked tubular joints can be studied using Fracture mechanics [5]. The behavior of each tubular joint is unique in a way as many variables can affect the joint behavior, i.e. the crack location, geometric dimensions, joint type, loading modes, stress ratio, weld profile, and boundary conditions [6]. Full-scale laboratory testing of cracked tubular joints is expensive and time-consuming while numerical simulation of fracture process of tubular joints has been a major task in recent research. The advancement of numerical methods and computational power made it possible to assess cracked tubular joints considering the uniqueness of each joint. Numerical methods such as finite element

methods (FEM), extended finite element method (XFEM) and boundary element method (BEM) are typically used for fracture mechanics analysis. FEM is widely used for stress analysis and fatigue life estimation of cracked tubular joints [7-16], while applications for cracked tubular joints with the use of XFEM has not been identified. BEM was encountered only once by Borges et al. [17] for comparison between SIFs for cracked tubular joints estimated from FEM and BEM.

This paper presents a review of the residual life estimation of cracked tubular joints using numerical methods. Based on the observations discussed above, this paper focuses on the numerical modelling of fatigue life using FEM. In general, the numerical models are based on the assumptions of constant-amplitude fatigue loading with crack propagating from a given initial crack within the domain of linear elastic fracture mechanics (LEFM).

2. Fatigue life evaluation of cracked tubular joints

The assessment of structures using fracture mechanics approach requires sizing of a crack-like defect. The size of the crack is determined mainly by the inspection method used. If the crack cannot be observed, the crack size can be assumed as the largest undetectable crack. Once the initial crack size is determined, fracture mechanics can be employed to evaluate the crack propagation until the onset of unstable crack extension, at which the structural element will lose its structural capacity. Fracture assessment of the component rely on the techniques of LEFM or elastic plastic fracture mechanics (EPFM) depending on material properties and plate thickness [1]. The fracture mechanics approach provides mathematical relationship between three critical variables, namely, flaw size, stresses in the vicinity of the crack and toughness.

Fracture mechanics analysis of tubular joints is demanding. The tubular joint geometry with boundary conditions induce mixed-mode loading of the crack [18]. In this respect, the detailed analysis of stresses requires three-dimensional models of the joint [1, 2]. In the vicinity of the crack, the size of the finite elements must be comparable to the size of the crack increments, thus the meshing procedure becomes challenging.

Conventional FE approach can be divided into four main steps: (1) development of numerical model with an initial crack-like defect; (2) evaluation of fracture mechanics parameters; (3) estimation of crack propagation rate, crack propagation direction and selecting crack increment size; (4) updating the numerical model with the new crack front. These steps are repeated for successive crack sizes until the structure loses its load carrying capacity as shown in Figure 1.

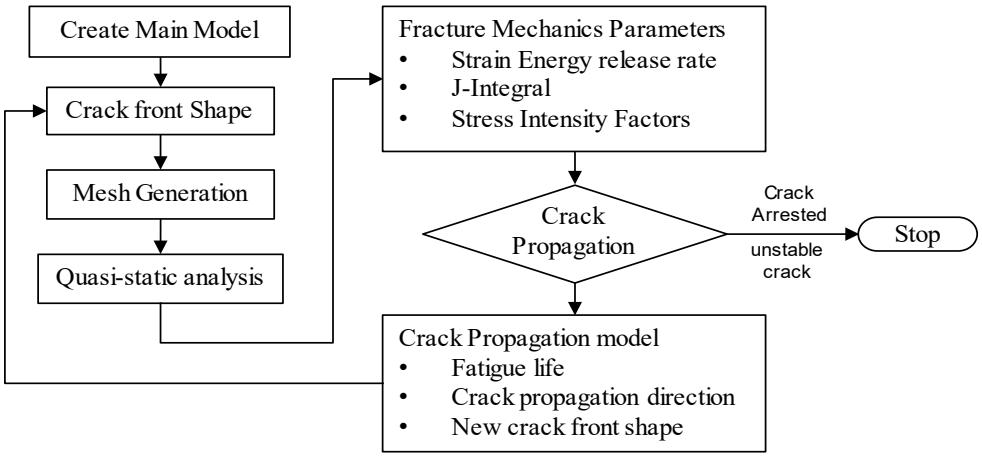

Figure 1. Conventional FE approach for fatigue life estimation of cracked tubular joints [19].

3. Numerical model generation

Numerical modelling of cracked tubular joints for fatigue life assessment is a computational expensive task as computational procedures are repeated for each successive crack increment. In this literature study, only simple tubular joints with focus on T/Y- joints are considered.

3.1. Type of finite elements

Stress concentration is generated at crack-tip and mesh refinement is needed in the vicinity of the crack-tip to capture the large stress and strain gradients. For sharp crack-tip, an inverse square root singularity exists. The singularity must be considered for reliable analysis of stress. First attempt in modelling tubular T-joint with a shallow weld crack was carried out using a wedge-shaped singular element [20]. The element was obtained by collapsing faces of 8-node brick element and choosing a displacement interpolation function. Elements with 6, 5 and 4 faces produced from the brick element with the displacement interpolation function updated accordingly. Later Rhee el al. [7] modelled K-joint for fatigue crack growth analysis using singular elements for crack-tip with quarter point.

The most common finite elements used in recent literature are isoparametric elements with quadratic shape functions. These elements can represent curved shapes with small number of elements. To capture crack-tip singularities, solid elements such as those shown in Figure 2(a) – (d) are typically used. While 20-node hexahedral elements (Figure 2(a)) are generally used for structured mesh, 10-node tetrahedral elements (Figure 2(b)) can be used for unstructured mesh [18, 21]. In the vicinity of a sharp crack-tip, square root stress singularity can be obtained by collapsing the 20-node hexahedral element (Figure 2(c)) to 15-node wedge elements and moving the mid-side nodes to quarter points.

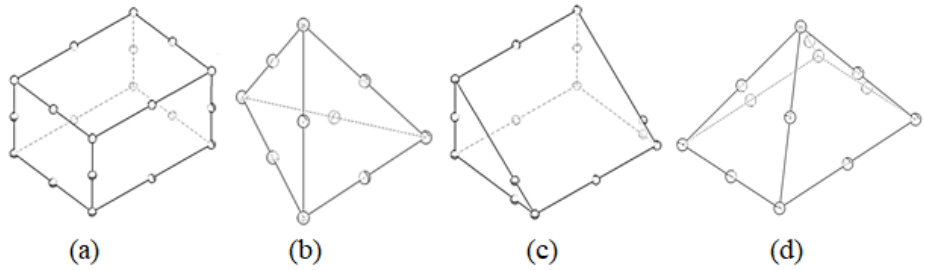

Figure 2. Typical solid mesh elements (a) 20-node hexahedral element (b) 10-node tetrahedral element (c) collapsed quarter-point hexahedral element and (d) 20-node pyramid – collapsed hexahedral.

The usage of tetrahedral elements allows decreasing the number of elements through thickness, away from sensitive areas, which reduces the computational time. On the other hand, this approach requires dense mesh around the crack-tip to produce convergence of the high stress-gradient expected and to accurately evaluate stress intensity factors (SIF).

3.2. Mesh Generation

Finite element simulation can be facilitated using an automated mesh generation system to handle the remeshing procedure during simulation. Many researches developed their meshing algorithms to carry out the remeshing procedure [9-12, 15, 16, 22]. Generally, the mesh generation of cracked tubular joints can be divided into two groups, structured mesh approach and unstructured mesh approach.

3.2.1. Structured mesh approach. One of the first automated structured mesh approaches was developed by Bowness and Lee [11, 23]. Their algorithm was used to assess cracked T-Joints considering a doubly curved semi-elliptical crack emanating from the weld toe. The algorithm is of 'building block' nature starting with a discretization of a plain plate containing a semi-elliptical crack as presented in Figure 3(a) below. A modelling sequence, as illustrated in Figure 3 (a) – (f) [23], is implemented using the following steps:

a) Adding an attachment to the plain plate,
b) Mapping to provide a weld profile at its base,
c) Making the mesh curved round 90° to become a brace,
d) Mapping the main plate into a square,
e) Making the main plate curved around the crack plane by 90° to form the chord,
f) Finally, adding the rest of the chord to form a quarter tubular T-joint.

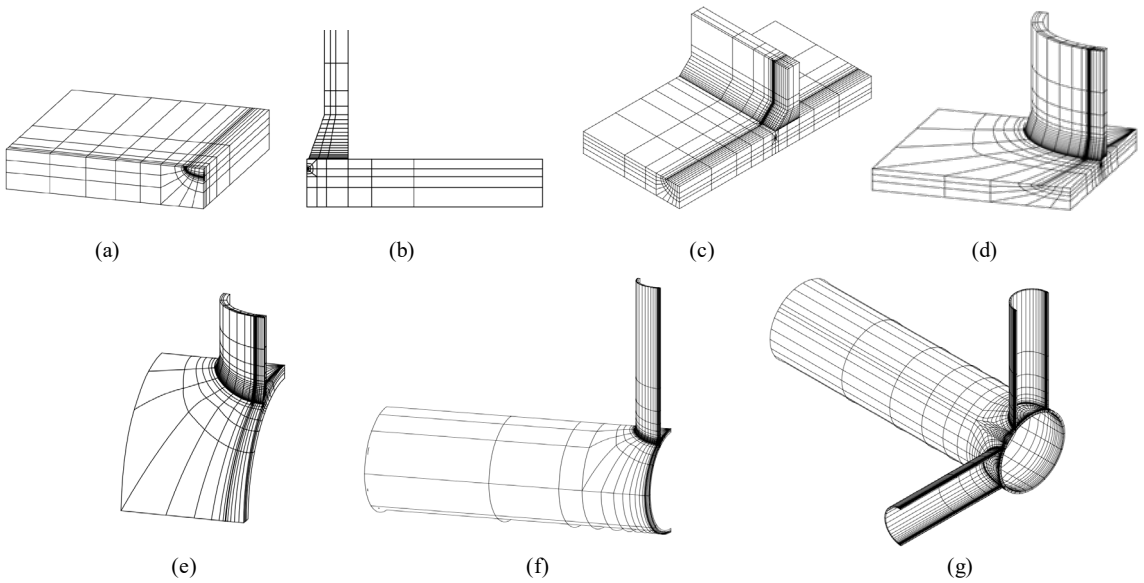

Figure 3. Bowness and Lee modelling sequence, (a) quarter plain plate with half surface crack, (b) mapped attachment and weld profile, (c) half T-butt joint, (d) curved T-butt plate to form the brace and weld, (e) chord-brace assembly from curved configuration d, (f) quarter T-joint, (g) Final mesh.

Lie et al. [15] developed a structured meshing algorithm to study cracked T/Y-shape joints. The algorithm creates a surface crack block which is divided into three parts: (1) crack tube part, where the crack front is located, (2) part which acts as transition from crack tube to the rest of the model and (3) part which contains the crack faces. Then it creates the chord-brace intersection zone by double mapping a flat vertical attachment and fillet weld.

3.2.2. Unstructured mesh approach. The advantage of unstructured mesh approach is that no focus mesh is required around the crack-tip, which significantly reduces the time and effort needed to develop the meshing algorithms. Yagi et al. [16] used tetrahedral elements to study surface-cracked T-shape joints. The approach was based on creating an intact three-dimensional CAD model for the joint then inserting an initial semi-elliptical surface crack at the weld toe. Solid elements meshing with quadratic tetrahedral elements were applied with double nodes on the crack surface to simulate a seam crack. The meshing procedure was repeated for each crack increment.

3.3. Weld profile

Typical tubular brace to chord joints are full penetration butt welded, characterised by changing weld profile from crown heel to crown toe due to the projection of the tubular brace on the tubular chord. It was found that weld toe radius and weld angle affect the SIF [24, 25]. Hence, it is important to model the weld profile if cracks emanate from weld toe or root. The influence of the weld leg size and weld angle to the SIF is prominent for smaller crack depth [26]. Typical weld details across the joint are shown in Figure 4.

Lie et al. [15] and Bowness et al. [11, 23] map the attachment to include fillet weld, then the attachment and the weld is being curved to simulate the brace. Mapping fillet weld does not conform with butt-weld profile at the saddle location see Figure 4, especially for joints with high brace diameter to chord diameter ratio. However, SIF at the crack deepest point was in a good agreement with experimental work. The effect of weld profile is not dominant at the crack deepest point. In fact, it will be more dominant towards the crack corners.

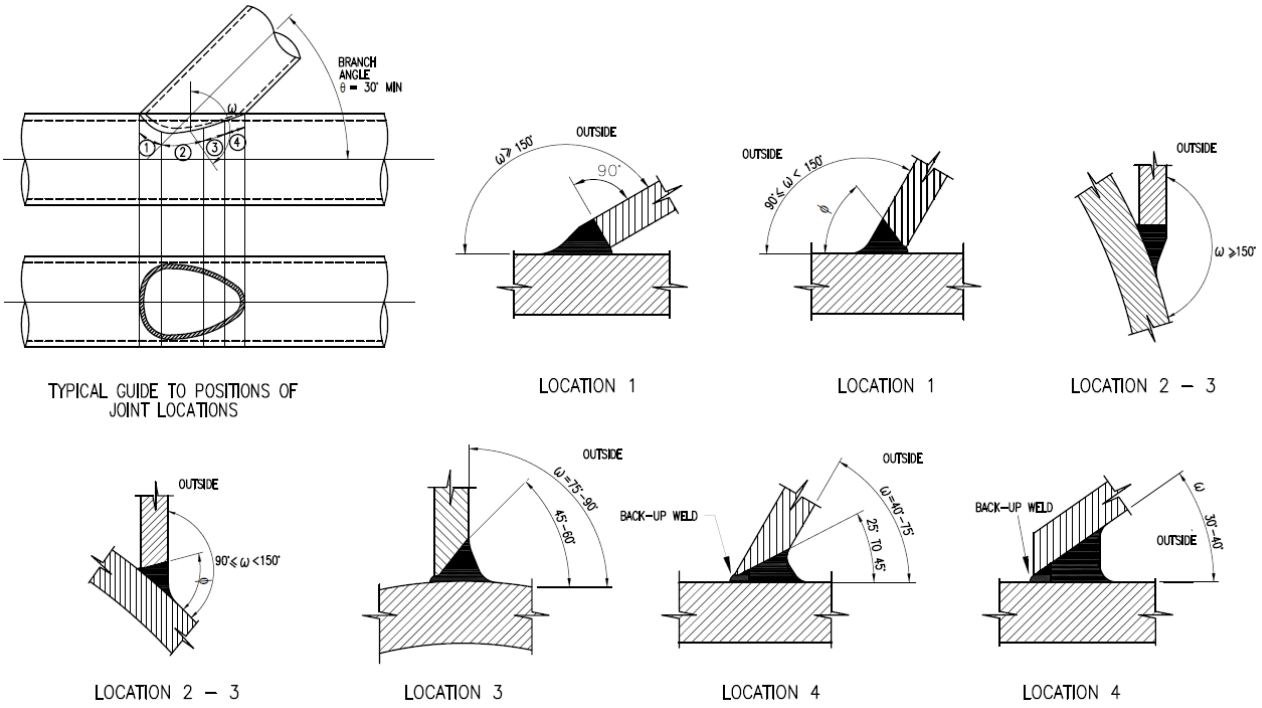

Figure 4. Weld profile of a typical offshore tubular joint.

3.4. Crack front shape

Crack front shape is generally double curved, and difficult to describe and predict [27]. Under fatigue loading, cracks emanate from the surface then evolve to through-thickness cracks. Through the literature, surface cracks are idealized as semi-elliptical cracks [14, 25, 28, 29]. In reality, cracks initiate at multiple locations and then coalescence to form a part-elliptical shape [30, 31]. Qian et al [3] showed variation up to 7% between semi-elliptical crack shape and the true-crack front profile. The variation translates to more than 20% in the crack growth rate.

Modelling surface cracks is more complex than modelling through-thickness cracks. For surface cracks, if the cracks exist on the chord side, the crack surface will be of inclined plane and the crack geometry will lead to mixed-mode condition [32]. The crack surface was assumed to be perpendicular to the free surface all the time by YongBo et al. [14]. While Bowness et al. [33] showed that the crack surface is not perpendicular to the free surface and that it curves away from the axis perpendicular to the free surface by a fourth degree polynomial function.

3.5. Singularities in cracked bodies.

For a surface crack in a homogeneous material not restrained by a weld, two sources of stress field singularity exist along the crack-front, near field stress singularity and vertex stress singularity. Near field stress singularity extend over most of the crack front and diminish to zero at the corner points. Vertex stress singularity exists at the corner points. The power of the vertex stress singularity is weaker than the near field stress singularity. The power changes monotonically from -0.5 at the interior to -0.37 at the free surface [34]. The weaker stress singularity at the corner point eventually leads to drop in the SIF from the interior of the crack front. Practical approach can be used by extrapolating the SIF from the interior part to the corner point and use it to evaluate the crack growth rate and direction [16]. Vertex singularity is a function of the material Poisson's ratio and the angle between the crack front and the free surface β. If the angle is small then SIFs tends to zero at the corner point, while if the angle is large SIFs tends to infinity. The crack front is observed to intersect the free surface at a critical angle β_c for which SIFs are finite. The critical angle is a function of material Poisson's ratio (equation 1) and type of loading. For steel materials with $\nu = 0.3$, under mode I loading, the crack front intersects the free

surface at a critical angle of 100.4° and an angle of 67.0° for antisymmetric loading [27]. Hence, the assumption that surface cracks are of semi-elliptical form (Figure 5) may not be valid.

The critical angle β_c for mode I case is given by:

$$\beta_c = \tan^{-1}\left(\frac{\nu - 2}{\nu}\right) \quad (1)$$

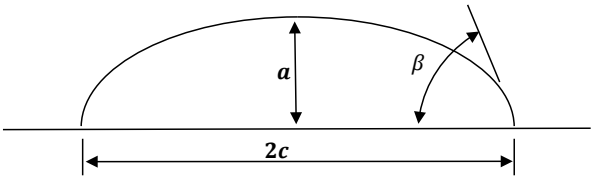

Figure 5. Part-elliptical surface crack [27].

4. Stress intensity factor evaluation methods

For crack-like defects in structural components under loading, there will be relative movement between the two crack faces, and stress field will develop at the crack tip. SIF describes the stress field in the vicinity of the crack and represents the tendency of the crack to advance under static loading conditions. As a minimum, to accurately determine the SIF for a crack in a tubular joint, the following parameters must be taken into account: crack position, crack front shape, coalescence of cracks, variation of stresses, and residual stresses.

Analytical solutions of SIF for a three-dimensional surface crack in tubular joints do not exist in the literature. Approaches that can be used to determine the SIF of cracked tubular joints are; classical solutions for idealized geometries modified to represent tubular joints, Semi-empirical methods based on full-scale testing or numerical methods. Numerical methods are the only approaches that can take into account all the parameters required to accurately determine the SIF [1].

The evaluation of SIF using conventional FEM requires that the mesh conform to the crack tip geometry. The accuracy of stress intensity factors depended on the quality of the FE mesh [3, 15-17, 26]. Several numerical methods exist for the evaluation of SIF in three-dimensional cracked components, the methods can be divided into the two main categories: (1) stress and displacement matching methods and (2) energy-based methods [19].

4.1. Stress and displacement matching methods.

These methods match the stress or displacement field calculated by the FEM with the analytical stress or displacement field which contain the SIF. For instance, using the *displacement extrapolation technique* [7, 8, 11, 15, 22, 23] the SIF is estimated from the elastic displacements behind the crack-tip. Then the displacements are extrapolated along a radial path to the weld toe as illustrated in Figure 6. For plane strain conditions, K_I can be estimated from the following extrapolation [35].

$$K_I = \lim_{r \to 0}\left[\frac{Eu_y}{4(1-\nu^2)}\sqrt{\frac{2\pi}{r}}\right] \quad (\theta = \pi) \quad (2)$$

where K_I denotes SIF for mode I loading, r is the radial distance between the crack-tip and the point of displacement extrapolation, E is Young's modulus of elasticity, ν is Poisson's ratio, and θ is the angle between the crack plane and the point of displacement extrapolation.

For plane stress loading, K_I can be estimated from the following expression.

$$K_I = \lim_{r \to 0}\left[\frac{Eu_y}{4}\sqrt{\frac{2\pi}{r}}\right] \quad (\theta = \pi) \quad (3)$$

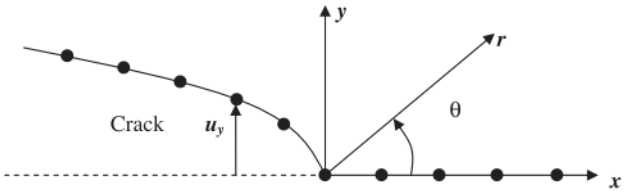

Figure 6. displacement field at crack tip [35].

4.2. Energy-based methods.

Energy-based methods relate the singular stress field to the energy release rate. The change in energy release rate associated with crack propagation can be evaluated by performing two numerical analyses, one with crack length a, and the other with crack length $a + \Delta a$. Energy-based methods are more-efficient than the stress and displacement matching methods, as energy is insensitive to mesh refinement.

As an energy-based method, the *virtual crack extension* (VCE) method was used [10, 15, 16, 23] based on the assumption that the energy release rate (G) for a growing crack from length a to $a + \Delta a$ is equivalent to the work needed to close the crack by Δa. It requires the calculation of stresses and displacements at the crack-tip. Numerical representation of VCE in a two-dimensional FE problem is shown in Figure 7.

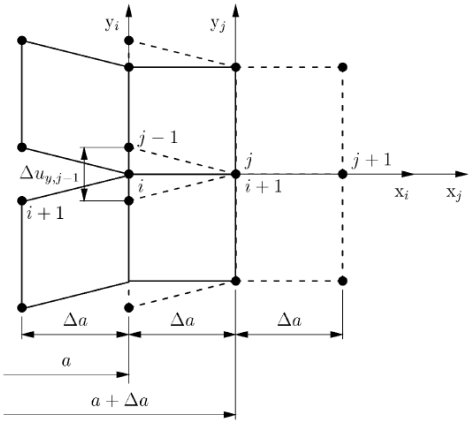

Figure 7. numerical representation of the virtual crack closure integral method [36].

Two stress or displacement calculations are required to evaluate the SIF using VCE for one crack configuration and the procedure can be numerically expensive. The analysis can be performed only once if the crack intervals Δa are small [35] and hereafter the procedure is called the modified virtual crack closure method [36].

Energy domain integral methods. It is the general framework for numerical analysis of J integral. For a rate-independent quasi-static fracture analysis, a single analysis is required to determine the energy release rate in the vicinity of a growing crack. J-integral is a function of the energy release rate associated with crack advance. The J-integral yields an accurate solution to the stress intensity factors within the LEFM domain, though it cannot easily used in the condition of mixed mode loading which is present in the tubular joints. In addition, J-integral lacks path independence at the crack corners because of the presence of two stress singularities, one caused by the crack-tip and the other caused by weld [14, 23].

5. Crack propagation models

Under static loading, the necessary condition for crack propagation is determined by material properties and the stress field in the vicinity of the crack expressed with SIF. Typical fatigue crack growth behaviour in metals can be described by a log-log curve of da/dN and ΔK as shown in Figure 8. da/dN is the crack growth rate and ΔK is the stress range expressed with SIF's $K_{max} - K_{min}$. The curve consists of three regions; the first region, includes the threshold value ΔK_{th}, below which the crack will not grow.

The second region describes the linear relation between log da/dN and log ΔK. In the third region the crack accelerates eventually until final failure of the joint.

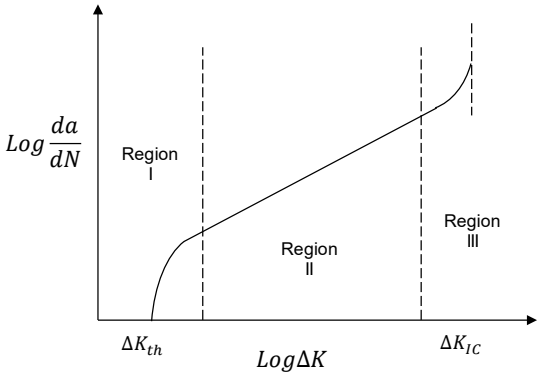

Figure 8. Typical fatigue crack growth curve

Paris-Erdogan proposed a power relation of the form;

$$\mathrm{da}/_{\mathrm{dN}} = \mathrm{C}\Delta\mathrm{K}_{\mathrm{eff}}{}^{\mathrm{m}} \tag{4}$$

where C and m are material constants, and $\Delta K_{eff} = K_{max} - K_{op}$, K_{max} is the maximum stress intensity, and K_{op} is the stress intensity at which the crack opens.

Paris-Erdogan law was being used extensively in cracked tubular joints literature [3, 14, 16, 26, 37, 38]. Paris-Erdogan law is insensitive to the stress ratio R defined by K_{min}/K_{max} and considers only region II (Figure 8). The most common expression to describe fatigue crack growth is called NASGRO [39].

$$\frac{\mathrm{da}}{\mathrm{dN}} = \mathrm{C}\Delta\mathrm{K}^{\mathrm{m}} \frac{\left(1 - \frac{\Delta\mathrm{K}_{\mathrm{th}}}{\Delta\mathrm{K}}\right)^{\mathrm{p}}}{\left(1 - \frac{\mathrm{K}_{\mathrm{max}}}{\mathrm{K}_{\mathrm{Ic}}}\right)^{\mathrm{q}}} \tag{5}$$

where $C,\ m,\ p,\ and\ q$ are material constants and K_{1c} is fracture toughness

NASGRO expression considers the three regions for crack propagation rate and is sensitive to the stress ratio. The number of cycles (N) required for a given increase in crack size from an initial length a_o to a final length a_f is given by:

$$\mathrm{N} = \int_{\mathrm{a_o}}^{\mathrm{a_f}} \frac{\mathrm{da}}{\mathrm{f_1}(\Delta\mathrm{K})} \tag{6}$$

5.1. Fracture criterion

Under mixed-mode loading condition, the use of equivalent stress intensity K_{eq} is necessary to consider the effect of K_I, K_{II} and K_{III}. Cracks can grow under the following conditions.

$$\mathrm{K_{th}} < \mathrm{K_{eq}} \leq \mathrm{K_{IC}} \tag{7}$$

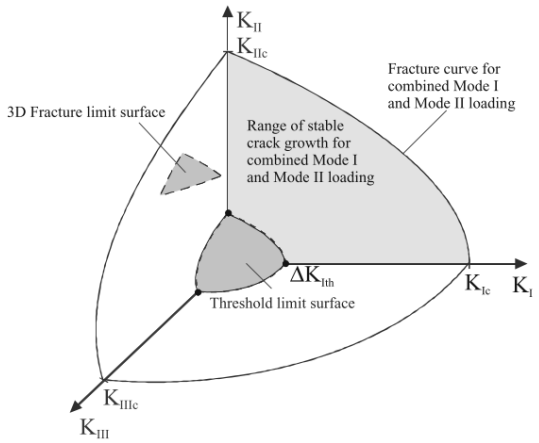

Figure 9. Mixed mode loading with fracture limit and threshold surface [40].

Rhee [18] considered the effect of mixed-mode on the SIF by converting the energy release rate relation which is given by

$$\frac{\Delta K_{eq}^2}{E} = G = \frac{1-\upsilon^2}{E}\left({K_I}^2 + {K_{II}}^2 + \frac{{K_{III}}^2}{1-\upsilon}\right) \tag{8}$$

Rhee [41] proposed another parameter to describe the effect of mixed-mode on the SIF and it was used by Qian et al. [3], YongBo et al. [15] and Chiew et al. [3, 12, 14].

$${K_{eq}}^2 = \frac{{K_I}^2 + {K_{II}}^2 + {K_{III}}^2}{1-\nu} \tag{9}$$

Another criterion was proposed by Richard [42], which is based on the MTS criterion,

$$K_{eq} = \frac{K_I}{2} + \frac{1}{2}\sqrt{{K_I}^2 + 4(1.155K_{II})^2} \tag{10}$$

5.2. Crack propagation direction

Crack propagation in solids under mixed-mode loading tends to eliminate mode II and mode III loading conditions. For crack propagating under mode I and mode II, the crack tends to eliminate mode II condition by adopting a crack path direction corresponding to the Mode I loading. When a crack propagates under mixed-mode loading, the crack front tends to both deflect and twist the orientation of the crack to comply with mode I loading [32, 33].

Crack propagation direction criteria can be divided into two groups, the first group describes the crack propagation direction at each point on the crack front by using the values of the SIFs and can be called *local type criteria* [32]. Example of these criteria is the MTS criterion, proposed by Erdogan and Sih [43] and extended to three dimensions by Schollmann et al. [44] and simplified by Richard et al. [45]. The second group describe the crack propagation by considering the mean value of SIFs along the whole crack front and can be called *global type criteria*. Examples of these criteria are the criteria by Pook [27] and Lazarus et al. [32, 46, 47]. Crack deflection and crack twisting angle by Richard et al. [45] can be described as;

$$\theta = \mp\left[A\frac{|K_{II}|}{K_I + |K_{II}| + |K_{III}|} + B\left(\frac{|K_{II}|}{K_I + |K_{II}| + |K_{III}|}\right)^2\right] \tag{11}$$

where $\theta < 0°$ for $K_{II} > 0$ and $\theta > 0°$ for $K_{II} < 0$ and $K_I \geq 0$.

$$\psi = \mp\left[C\frac{|K_{II}|}{K_I + |K_{II}| + |K_{III}|} + D\left(\frac{|K_{II}|}{K_I + |K_{II}| + |K_{III}|}\right)^2\right] \tag{12}$$

where $\psi < 0°$ for $K_{III} > 0$ and$\psi > 0°$ for $K_{III} < 0$ and $K_I \geq 0$.$A = 140°$, $B = -70°$, $C = 78°$ and $D = -33°$

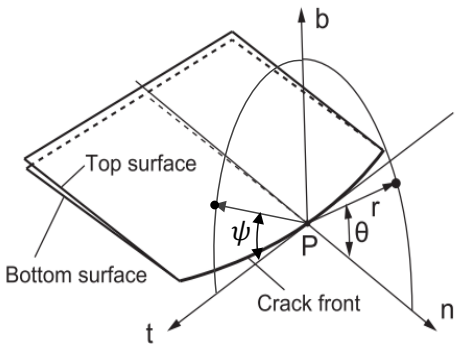

Figure 10. Polar coordinates at point P along the crack front with crack deflection angle $\boldsymbol{\theta}$ and crack twisting angle $\boldsymbol{\psi}$ [42]

Yagi et al. [16] used the three dimensional MTS criterion proposed by Gerstle [48], and formulated the crack deflection angle in the form of;

$$\theta = 2\tan^{-1}\left[\frac{-2\Delta K_{II}}{\Delta K_{Ieq} + \sqrt{(\Delta K_{Ieq})^2 + 8(\Delta K_{II})^2}}\right] \tag{13}$$

where ΔK_{Ieq} is an equivalent SIF range including the mode-III effect, and given by;

$$\Delta K_{Ieq} = \Delta K_I + B|\Delta K_{III}| \tag{14}$$

where B an empirically determined factor = 1.0.

Criterion by Pook [27] can be calculated in a step-by-step process.

$$K_I \sin\theta = -K_{II}(3\cos\theta - 1) \tag{15}$$

$$K_{vI,II} = \frac{0.83K_I + \sqrt{0.4489{K_I}^2 + 3{K_{II}}^2}}{1.5} \tag{16}$$

$$\tan 2\psi = \frac{2K_{III}}{K_{vI,II}(1-2\upsilon)} \tag{17}$$

In Pook's criterion the equivalent stress intensity K_{eq} considers the effect of K_I, K_{II} and K_{III}. K_{eq} can be described by the following relation.

$$K_{eq} = \frac{K_{vI,II}(1+2\upsilon) + \sqrt{{K_{vI,II}}^2(1+2\upsilon)^2 + 4{K_{III}}^2}}{2} \tag{18}$$

Another crack propagation criterion in use is the minimum strain energy criterion as presented by Sih [49, 50]. The crack is then assumed to propagate in the direction of minimum strain energy density, S, expressed as;

$$S = \frac{a_{11}{K_I}^2 + 2a_{12}K_IK_{II} + a_{22}{K_{II}}^2 + a_{33}{K_{III}}^2}{\pi} \tag{19}$$

where a_{ij} are coefficients relating crack deflecting angle θ, elastic modulus and Poisson's ratio.

5.3. Crack increment step

Typically, the crack growth increment and direction are calculated for each node at the crack front based on SIFs, and the crack is then extended for the next step. The number of nodes at the crack front is kept the same for all increments [16, 29].

Crack increment step is influential to fatigue life estimation. There are two approaches for crack increment step; the first is based on a constant crack length increment and the second is based on a constant number of cycles increment (Figure 11). Due to the geometry and loading of the tubular joints, it is expected that SIF will vary along the crack front. As a result, the crack will not advance equidistantly along the crack front for the same number of cycles. Therefore, for accurate crack propagation estimation, crack increment step based on constant number of cycles may be used.

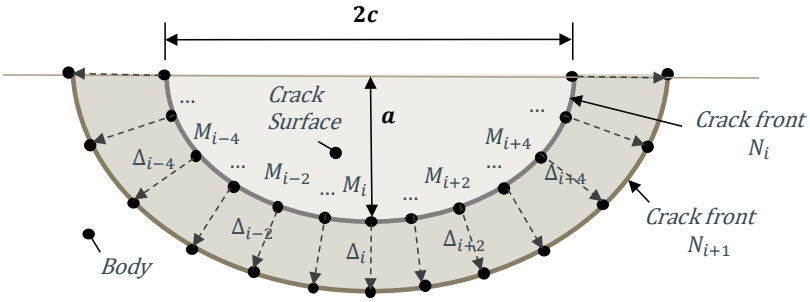

Figure. 11. Surface crack and schematic illustration of the crack propagation [29].

6. Conclusion

The objective of this paper is to provide an overview of the fatigue life estimation of cracked tubular joints using fracture mechanics and FEM. With respect to mesh generation, the methods proposed over the last two decades considered two different types, structured and unstructured mesh generation. Structured mesh generation is considered as systematic approach and provide reliable results. However, the method is limited to simple geometries. Unstructured mesh has the potential to be extended to more complex geometries due to the less effort needed for automation and model creation. To the knowledge of the authors the meshing algorithm which accommodate the automatic transition from surface cracks to through-thickness cracks has not yet been implemented and documented.

Through the literature, surface cracks are idealized as semi-elliptical cracks. In reality, cracks initiate at multiple locations and then coalescence to form a part-elliptical shape. That idealization may cause a discrepancy in crack growth rate up to 20%. The crack front in tubular joints is of double curved nature and subjected to mixed mode loading due to the joint geometry. The assumptions for calculation of crack propagation angle was limited to the use of MTS criterion. The MTS criterion provides crack deflection and crack twisting angles for each point on the crack front which fits well with meshing algorithms.

The methods for SIF evaluation of cracked tubular joints, found in the literature were displacement extrapolation, VCE and the domain integral methods. VCE method for a crack configuration requires calculations of two stresses or two unknown displacements to evaluate the SIF. The method is regarded numerically expensive. The domain integral method performs poorly under mixed-mode loading conditions and at crack corners it is not path independent. The displacement extrapolation method is thus recommended for SIF evaluation of cracked tubular joints

The advantage of the LEFM is that each parameter that may affect the fatigue life may be assessed individually and it is possible to extend the test data to other conditions than those under which the tests were performed [1]. However, none of the studies reviewed considered the influence of the following parameters on the residual fatigue life of cracked tubular joints: residual stresses, stress ratio effects, environment (air, seawater) exposures and variable amplitude loading.

The complexity of evaluating the residual fatigue life of cracked tubular joints is due to the inherent shortcomings of FEMs, including;

- Finite element discretization at crack tip area in 3D is complex.
- The assumption of crack propagation direction prior to calculation of SIF.
- Explicit definition of the crack front.

The literature study shows that the XFEM can overcome the limitations listed above. The method is independent of crack initiation or propagation and it can provide solution-dependent crack initiation and propagation path. The accuracy of XFEM is however not tested with applications for tubular joints.

Acknowledgements
This work is part of a PhD study supported by the Norwegian Ministry of Education and Research. The financial support is acknowledged.

References

[1] CIRIA Underwater Engineering Group 1985, Design of tubular joints for offshore structures, UEG, London
[2] Zhang Y H and Stacey A 2008 Review and assessment of fatigue data for offshore structural components containing through-thickness cracks *Int. Conf. Offshore Mech. Arc. Eng.*, Estoril, Portugal
[3] Qian X and Nguyen C T 2012 Prediction of the fatigue crack propagation in large-scale tubular joint specimens *22nd Int Offshore Polar Eng. Conf.*, Rhodes, Greece
[4] Sharp J V, Stacey A and Wignall C M 1998 Structural integrity management of offshore installations based on inspection for through-thickness cracking 1*7th Offshore Mech. Arct. Eng. Conf.*, Lisbon, Portugal
[5] Rhee H C and Kanninen M F 1988 Opportunities for application of fracture mechanics for offshore structures *Appl. Mech. Rev.* **41** 23-35
[6] Haswell J and Hopkins P 1991 A review of fracture mechanics models of tubular joints Fatigue *Fract. Eng. Mater. Struct.* **14** 15-29
[7] Rhee H C 1989 Fatigue crack growth analyses of offshore structural tubular joints *Eng. Fract. Mech.* **34** 1231-9
[8] Laham S and Fm B 1997 The ultimate strength of cracked tubular K-joints
[9] Cao J J, Yang G J, Packer J A and F.M B 1998 Crack modeling in FE analysis of circular tubular joints *Eng. Fract. Mech.* **61** 537-53
[10] Bowness D and Lee M M K 2002 Fracture mechanics assessment of fatigue cracks in offshore tubular structures: HSE Books
[11] Lee M M K and Bowness D 2002 Estimation of stress intensity factor solutions for weld toe cracks in offshore tubular joints *Int. J. Fatigue.* **24** 861–75
[12] Chiew S P, Lie S T, Lee C K and Huang Z W 2003 Parametric equations for stress intensity factors of cracked tubular T&Y-joints *13th Int. Offshore Polar Eng. Conf.*, Honolulu, Hawaii, USA
[13] Lie S T, Lee C K and Wong S M 2003 Model and mesh generation of cracked tubular Y-joints *Eng. Fract. Mech.* **70** 161–84
[14] Yongbo S and Tjhen L S 2005 Parametric equation of stress intensity factor for tubular K-joint under balanced axial loads *Int. J. Fatigue.* **27** 666-79
[15] Lie S T, Li T and Shao Y B 2016 Stress intensity factors of tubular T/Y-joints subjected to three basic loading *Adv. Steel Constr.* **12** 109-33
[16] Yagi K, Tanaka S, Kawahara T, Nihei K, Okada H and Osawa N 2017 Evaluation of crack propagation behaviors in a T-shaped tubular joint employing tetrahedral FE modeling *Int. J. Fatigue.* **96** 270-82
[17] Borges L, Chiew S P, Nussbaumer A and Lee C K 2012 Advanced numerical modeling of cracked tubular K joints: BEM and FEM comparison *J. Bridge Eng.* **17** 432-42
[18] Rhee H C 1986 The behavior of stress intensity factors of weld toe surface flaw of tubular X-joint *Offshore Technol. Conf.*, Housten, Texas
[19] Branco R, Antunes F V and Costa J D 2015 A review on 3D-FE adaptive remeshing techniques for crack growth modelling *Eng. Fract. Mech.* **141** 170-95

[20] G.S H, M A and Munaswamy K 1985 Analysis of tubular joint with weld toe crack by finite element methods Communications in *appl. numer. methods.* **1** 325-31
[21] Du Z Z and Hancock J W 1989 Stress intensity factors of semi-elliptical cracks in a tubular welded joint using line springs and 3D finite elements *J. Pressure Vessel Technol.* **111** 247-51
[22] Burdekin F M, Yang G J and Cao J J 1998 Assessment of fracture strength of cracked tubular joints, HSE Books, Manchester
[23] Bowness D and Lee M M K 1995 The development of an accurate model for the fatigue assessment of doubly curved cracks in tubular joints *Int. J. Fract.* **73** 129-47
[24] Niu X, Glinka G 1987 The weld profile effect on stress intensity factors in weldments *Int. J. Fract.* **35** 3-20
[25] Delft D R V V, Dijkstra and Snijder H H 1986 The calculation of fatigue crack growth in welded tubular joints using fracture mechanics *Offshore Technol. Conf.*, Houston, Texas, USA
[26] Lie S T, Chiew S P, Lee C K and Huang Z W 2004 Fatigue performance of cracked tubular T joints under combined loads. II: numerical *J. Struct. Eng.***130** 572-81
[27] Pook L P 1995 On fatigue crack paths *Int. J. Fatigue.* **17** 5-13
[28] Skallerud B, Eide O I and Berge S 1990 Fatigue crack growth in complex tubular joints
[29] Tanaka S, Kawahara T and Okada H 2014 Study on crack propagation simulation of surface crack in welded joint structure *Mar. struct.* **39** 315-34
[30] Pang J H L, Tsang K S and Hoh H J 2016 3D stress intensity factors for weld toe semi-elliptical surface cracks using XFEM *Mar. struct.* **48** 1-14
[31] Pang J H L and Chew Y X 2014 Fatigue crack growth and coalescence algorithm starting from multiple surface cracks *Adv. Mater. Res.* **891-892** 1003-8
[32] Lazarus V, Buchholz F G, Fulland M and Wiebesiek J 2009 Comparison of predictions by mode II or mode III criteria on crack front twisting in three or four point bending experiments *Int. J. Fract.* **153** 141-51
[33] Bowness D and Lee M M K 1998 Fatigue crack curvature under the weld toe in an offshore tubular joint *Int. J. Fatigue.* **20** 481-90
[34] Shivakumar K N and Raju I S 1990 Treatment of singularities in cracked bodies *Int. J. Fract.* **45** 159-78
[35] Anderson T L 2017 Fracture mechanics: fundamentals and applications: CRC Press
[36] Schoollmann M, Fulland M and Richard H A 2003 Development of a new software for adaptive crack growth simulations in 3D structures *Eng. Fract. Mech.* **70** 249–68
[37] Shen W and Choo Y S 2012 Stress intensity factor for a tubular T-joint with grouted chord *Eng. Struct*. **35** 37-47
[38] Etube L S 2001 Fatigue and fracture mechanics of offshore structures vol 4 London: Professional Engineering Publ.
[39] Forman R G and Mettu S R 1990 Behavior of surface and corner cracks subjected to tensile and bending loads in Ti-6Al-4V alloy *NASA technical memorandum*: NASA
[40] Richard H A, Fulland M and Sander M 2005 Theoretical crack path prediction Fatigue Fract. *Eng. Mater. Struct.* **28** 3-12
[41] Rhee H C, Han S and Gibson G S 1991 Reliability of solution method and empirical formulas of stress intensity factors for weld toe cracks of tubular joints *Offshore Mech. Arct. Eng. Conf.* 441-52, New York
[42] Richard H A, Schramm B and Schirmeisen N H 2014 Cracks on mixed mode loading – theories, experiments, simulations *Int. J. Fatigue.* **62** 93-103
[43] Erdogan F and Sih G C 1963 On the crack extension in plates under plane loading and transverse Shear *J. Fluids Eng.* **85** 519-25
[44] Schöllmann M, Richard H A, Kullmer G and Fulland M 2002 A new criterion for the prediction of crack development in multiaxially loaded structures *Int. J. Fract.* **117** 129-41
[45] Richard H A, Schirmeisen N H, Fulland M and Sander M 2001 Experimental and numerical simulation of mixed mode crack growth Proc. *Int. Conf. biaxial/multiaxial fatigue fract.* 623-

30
[46] Lazarus V and Leblond J B 1998 Crack paths under mixed mode (I + III) or (I + II + III) loadings
[47] Lazarus V, Leblond J-B and Salah-Eddine M 2001 Crack front rotation and segmentation in mixed mode I+III or I+II+III. Part II: Comparison with experiments *J. Mech. Phys. Solids.* **49** 1421-43
[48] Gerstle W 1985 Finite and boundary element modelling of crack propagation in two and three dimensions using interactive computer graphics: Cornell University, PhD Thesis
[49] Sih G C 1974 Strain-energy-density factor applied to mixed mode crack problems *Int. J. Fract.* **10** 305-21
[50] Sih G C 1991 Mechanics of fracture initiation and propagation, Springer Netherlands.